ACS BIO & MED CHEM Au
AN OPEN ACCESS JOURNAL OF THE AMERICAN CHEMICAL SOCIETY

pubs.acs.org/biomedchemau

Article

Continuous Flow Synthesis of A2E Guided by Design of Experiments and High-Throughput Studies

Giulia Murbach-Oliveira, Kalpita Banerjee, Marcelo M. Nociari, and David H. Thompson*

Cite This: *ACS Bio Med Chem Au* 2022, 2, 297−306

Read Online

ACCESS | Metrics & More | Article Recommendations | Supporting Information

ABSTRACT: *N*-Retinylidene-*N*-retinylethanolamine (A2E) is the most studied lipid bisretinoid. It forms lipofuscin deposits in the retinal pigment epithelium (RPE), causing vision impairment and blindness in eye conditions, such as Stargardt's disease, cone-rod dystrophy, Best's macular dystrophy, and potentially age-related macular degeneration. Synthetic A2E is often used for inducing the accumulation of lipofuscins within the lysosomes of RPE cells in culture as an in vitro surrogate of retinal lipofuscin buildup, providing insights into the mechanisms of these eye conditions. Many reports describing the use of synthetic A2E employ material that has been prepared using a one-pot reaction of all-trans-retinal (ATR) and ethanolamine at room temperature for 48 h. We have revisited this synthesis by performing a design of experiments (DoE) and high-throughput experimentation workflow that was tailored to identify the most productive combination of the variables (temperature, solvent, and reagent equivalences) for optimization of A2E yield. Our DoE findings revealed that the interaction of ethanolamine with acetic acid and ATR was pivotal for the formation of A2E in high yield, indicating that imine formation is the critical step in the reaction. Armed with these results, we were able to optimize the method using a microfluidic reactor system before upscaling those conditions for continuous flow synthesis of A2E. This revised method enabled a more efficient production of material, from a reaction time of 48 h to a residence time of 33 min, with an accompanying yield improvement from 49 to 78%. Furthermore, we implemented a simple method to evaluate the quality of the A2E produced using optical spectroscopy and LC−MS characteristics to assure that the biological properties observed with A2E samples are not confounded by the presence of oxidized impurities that are commonly present in conventional A2E samples.

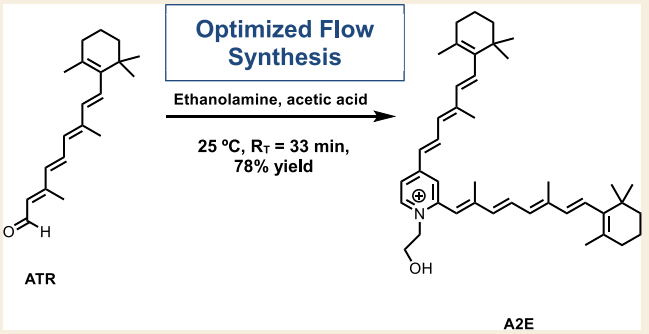

KEYWORDS: *N-retinylidene-N-retinylethanolamine, A2E, high-throughput experiment, continuous flow synthesis, Design of Experiments, Stargardt*

INTRODUCTION

The retinal pigment epithelium (RPE) is a cell monolayer that separates the retina from choroid circulation and is vital for the phagocytic recycling of photoreceptor waste, nutrient supply, ionic balance maintenance, and many other critical activities required for proper functioning of the retina.[1] Light detection by photoreceptors starts with the conversion of 11-cis-retinal, the prosthetic group sensitive to light in visual pigments, into its isomer, 11-trans-retinal (a.k.a., all-trans-retinal or ATR). ATR then needs to be replaced by another 11-cis-retinal to regenerate rhodopsin as part of the visual cycle process. All-trans or 11-cis retinaldehydes in photoreceptors tend to spontaneously dimerize into lipid bisretinoids that accumulate as retinal lipofuscin. Failures in ABCA4 function, a protein that flips retinaldehydes to the cytosol where deshydrogenases convert them into nontoxic retinols, exacerbate the formation of lipid bisretinoids.[2] As a consequence, lipid bisretinoids accumulate within the lysosomes of RPE cells, where they remain indefinitely because they are not susceptible to degradation by lysosomal enzymes. The accumulation of bisretinoid-rich lipofuscin in the RPE has been shown to induce cell death[3,27] and is believed to be a key culprit in the etiology of conditions such as Stargardt's disease, cone-rod dystrophy, Best's macular dystrophy, and potentially age-related macular degeneration (AMD).[4]

One of the most prevalent and most studied of such lipid bisretinoids is *N*-retinylidene-*N*-retinylethanolamine (A2E), a pyridinium quaternary amine comprising two retinaldehyde-derived moieties. The most cited article on the synthesis of A2E[5] uses ATR and ethanolamine in a one-step-synthesis (Scheme 1), with 1 equiv of acetic acid and ethanolamine in

Received: November 28, 2021
Revised: January 27, 2022
Accepted: January 28, 2022
Published: February 18, 2022

https://doi.org/10.1021/acsbiomedchemau.1c00060
ACS Bio Med Chem Au 2022, 2, 297−306

Scheme 1. A2E Synthesis as Described by Parish et al.[5]

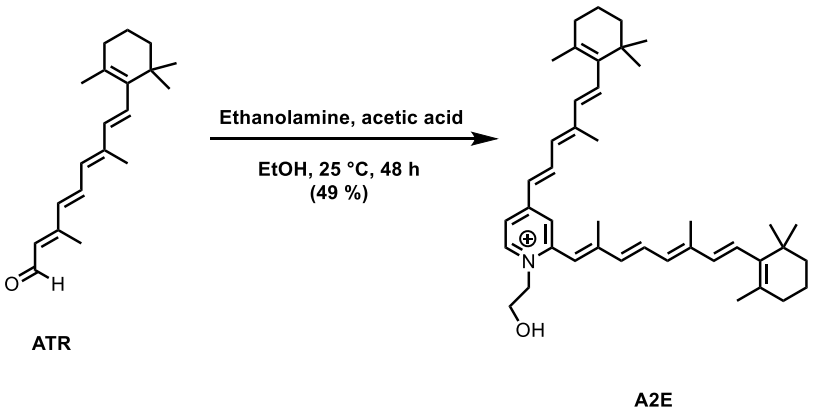

Scheme 2. Mechanism of A2E Formation from ATR, Ethanolamine, and Acetic Acid

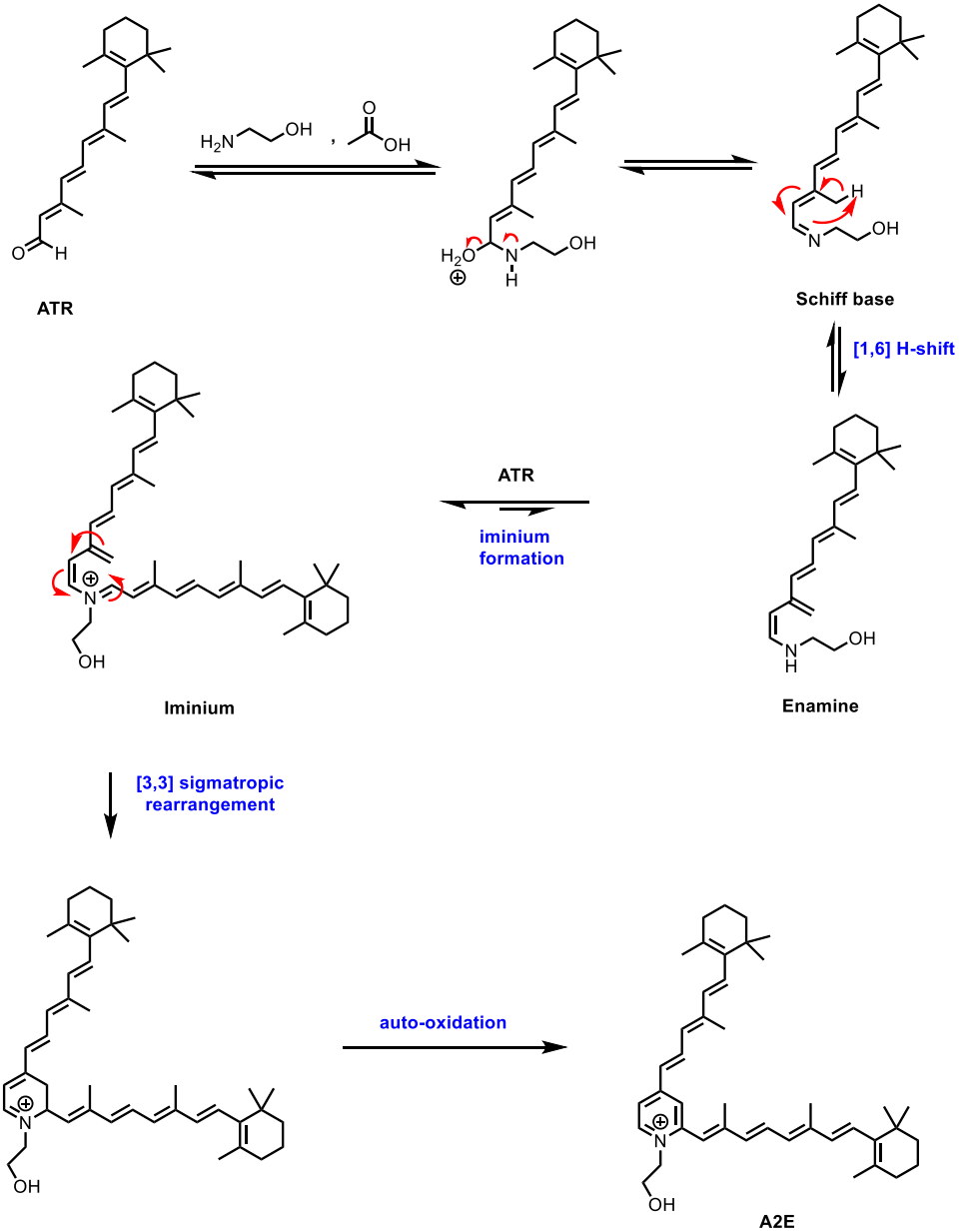

ethanol for 48 h at room temperature as the best condition for A2E product formation.

Scheme 2 shows that the first step in the transformation is the formation of ATR ethanolimine, followed by tautomeriza-

https://doi.org/10.1021/acsbiomedchemau.1c00060
ACS Bio Med Chem Au 2022, 2, 297−306

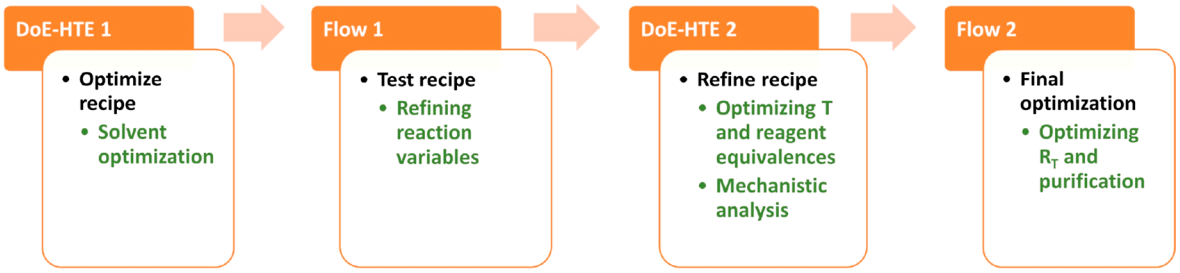

Figure 1. DoE-HTE-Flow workflow.

tion to an enamine in a [1,6] proton shift; subsequent addition of a second molecule of ATR produces an iminium ion intermediate. Rearrangement of the iminium ion and subsequent auto-oxidation generates A2E.[4,5]

Two aspects of the reaction mechanism are worth noting. In the first step, nucleophilic attack of the aldehyde by ethanolamine will be most favorable under alkaline conditions because in the presence of acid, the ethanolamine nitrogen will be protonated, thus reducing its nucleophilicity. Conversely, acid conditions favor the second step by protonating the aldehyde oxygen to produce the hydronium leaving group. As the imine formation is an equilibrium, it is necessary to have enough acid to promote the formation of the hydronium ion, but not so much that the nucleophile equilibrium favors full protonation of ethanolamine. Therefore, allowing time for the reaction of ATR with ethanolamine prior to the addition of acetic acid and investigation of the equivalence of acetic acid were viewed as the most crucial parameters to evaluate for optimizing reaction yield.

An additional factor to be considered in the planning of this reaction is the choice of solvent. Jin et al.[6] studied the effects of different solvents on the extraction of A2E from eyecups. They found that extraction with different solvents followed by high-performance liquid chromatography (HPLC) analysis of the extract revealed that A2E is not stable in THF, $CHCl_3$, or EtOH but is stable in methanol and dimethyl sulfoxide (DMSO). These findings motivated us to investigate the solvent as another parameter to be optimized.

Finally, we wanted to consider the role of temperature on reaction efficiency. As the conversion of ATR to A2E occurs under physiologic conditions, we sought to uncover whether the A2E yield would increase upon raising the reaction temperature from 22 to 37 °C and whether it would be improved at even higher temperatures.

Given these reaction variables of interest, we used a design of experiments (DoE) and high-throughput experimentation (HTE) strategy to improve the synthesis of A2E. DoE is a statistical methodology that aims to identify all major parameters involved in a reaction to reveal how those parameters interact because reaction parameters are rarely independent of each other.[7−9] Based on the DoE data obtained, the interplay of reaction parameters can be determined to guide the discovery of optimized conditions.

A key consideration in the DoE approach is the number of experiments to be performed.[10] For example, for a 3^2 factorial design, with two variables evaluated at three levels, a total of nine unique experiments are required, not including experimental replicates. The number of experiments required grows exponentially with the number of levels applied to the experiment. To simplify the execution of a large number of experiments and reduce costs, HTE is a valuable technique that is commonly used for data collection. HTE allows for the grouping of common operations so that a series of experiments can be rapidly performed in parallel at microscale. This approach also allows for the automation of procedures, such as liquid handling and data analysis, so that hundreds of experiments can be executed simultaneously and analyzed using quantitative techniques such LC−MS or semi-quantitatively by DESI-MS.[11−15] HTE also allows for facile and automated replication of experiments, making it the ideal pairing with the DoE approach, because the labor burden for implementing replicates does not increase considerably when the experiments are executed in a microscale format.[16,17]

Due to the light and oxidation sensitivity of A2E, we sought to apply the data inputs from our HTE campaign to continuous flow synthesis to provide better control over these parameters. Flow reactions involve the use of automated reagent delivery systems that are continuously mixed within a flow reactor and collected downstream with control over residence time, flow rate, reactor temperature, light exposure, and reaction O_2 content. The use of continuous flow methods allows for much better control over reaction parameters relative to batch syntheses due to the improved surface area-to-volume ratios in flow reactors that enable more efficient mixing and heat transfer. Microfluidic reactors also offer the advantages of safer handling and use of very small quantities of starting materials during the reaction optimization stage of process development. For preparative scales, the small-scale setup can be readily upscaled with the same control over mixing and heat transfer.[18]

RESULTS AND DISCUSSION

First Round of DoE and HTE

Figure 1 outlines the workflow pursued in the DoE-HTE optimization process. An initial 3^3 DoE was developed to generate a matrix with 27 experiments combining three variables (stoichiometry, solvent, and temperature) at three levels to discover the best reaction conditions and the variable interactions. We then used a Biomek i7 liquid handling robot to transfer the reagents in proportions required for the DoE into the respective wells of glass vial lined 96 well plates and sealed (Figure S1B).[11−15] The plates were then transferred to heating blocks set to 25, 37, and 100 °C and heated for 48 h (Figure S1C). After cooling to room temperature, the solutions were transferred from the three 96-well source plates to one 384-well daughter plate (Figure S1D,E) and stored at −80 °C until analysis. The Biomek i7 was then used to pin the solutions from the 384-well plate to a DESI-MS plate for MS analysis of all the reactions (Figure S1F,G).[11−15] Each reaction was performed in four replicates.

https://doi.org/10.1021/acsbiomedchemau.1c00060
ACS Bio Med Chem Au 2022, 2, 297−306

The DESI-MS signal intensities for the A2E product peak (592.45 m/z) for each of the 27 reaction conditions were corrected for background signal and the measured values (average of the four replicates for each experiment) scaled from 0−100% with respect to the highest product peak intensity observed (Table 1). Evaluation of the HTE findings from this initial 3^3 DoE revealed that the best conditions are 1 equiv of acetic acid at 37 °C in DMSO.

Table 1. HTE Results, First 3^3 DoE Experiment[a]

run	AA (eq.)	temp. (°C)	solvent	ion Intensity	% yield
1	0.1	25	EtOH	120	60.7
2	0.1	25	MeOH	25.2	12.7
3	0.1	25	DMSO	32.1	16.1
4	0.1	37	EtOH	72.4	36.4
5	0.1	37	MeOH	49.5	24.9
6	0.1	37	DMSO	52.8	26.5
7	0.1	100	EtOH	49.4	24.8
8	0.1	100	MeOH	26.4	13.3
9	0.1	100	DMSO	33.3	16.7
10	1	25	EtOH	28.4	14.3
11	1	25	MeOH	41.0	20.6
12	1	25	DMSO	31.2	15.7
13	1	37	EtOH	94.0	47.2
14	1	37	MeOH	77.5	38.9
15	1	37	DMSO	199	100
16	1	100	EtOH	34.9	17.5
17	1	100	MeOH	12.8	6.5
18	1	100	DMSO	28.5	14.3
19	10	25	EtOH	1.30	0.7
20	10	25	MeOH	44.2	22.2
21	10	25	DMSO	114	57.2
22	10	37	EtOH	92.0	46.2
23	10	37	MeOH	23.6	11.8
24	10	37	DMSO	159	79.8
25	10	100	EtOH	12.1	6.1
26	10	100	MeOH	35.3	17.7
27	10	100	DMSO	17.6	8.9

[a]AA = acetic acid. The normalized ion intensities are an average of the four replicates performed for each run. The yields are relative to the maximum ion intensity measured for product formation.

Utilizing Ellistat software, we generated contour plots to predict reaction gradient profiles (Figure 2). Inputting the ion counts measured in the DESI-MS experiment into the statistical analysis software, a projection of conditions was generated that would give higher ion counts based on the interaction of the factors studied. The contour plots suggest that the preferred conditions for this reaction are DMSO and 10 equiv of acetic acid at 25 °C.

Round 1: Continuous Flow Experiments

The results obtained from the HTE and DoE analyses were used to guide an initial screen of continuous flow conditions (Table S1). The flow setup (Figure S2) was designed so that ATR and ethanolamine would first engage in a T-mixer to initiate the imine formation reaction before it encountered acetic acid in the reactor chip. At the end of the reaction period, each sample was extracted and purified by column chromatography.

One indication of A2E purity is its UV−vis absorption spectrum. When pure, A2E will have two defined bands: one at approximately 336 nm and a more intense one near 439 nm.[5,19,20] The intensity of the 439 nm band is important because ATR, the synthetic precursor and a potential contaminant in the isolated A2E, contributes more to the sample absorbance at 330 nm than at 439 nm. Neither reaction generated a very pure A2E sample, even though their NMR spectra showed all the expected peaks for this compound. The difference between the UV−vis spectra obtained for the two experiments is remarkable, with the experiment run at lower temperature and higher acetic acid equivalency showing prominent bands at 333 and 432 nm. This observation suggests that both the decrease in temperature and increase in acetic acid equivalency lead to increased reaction yield.

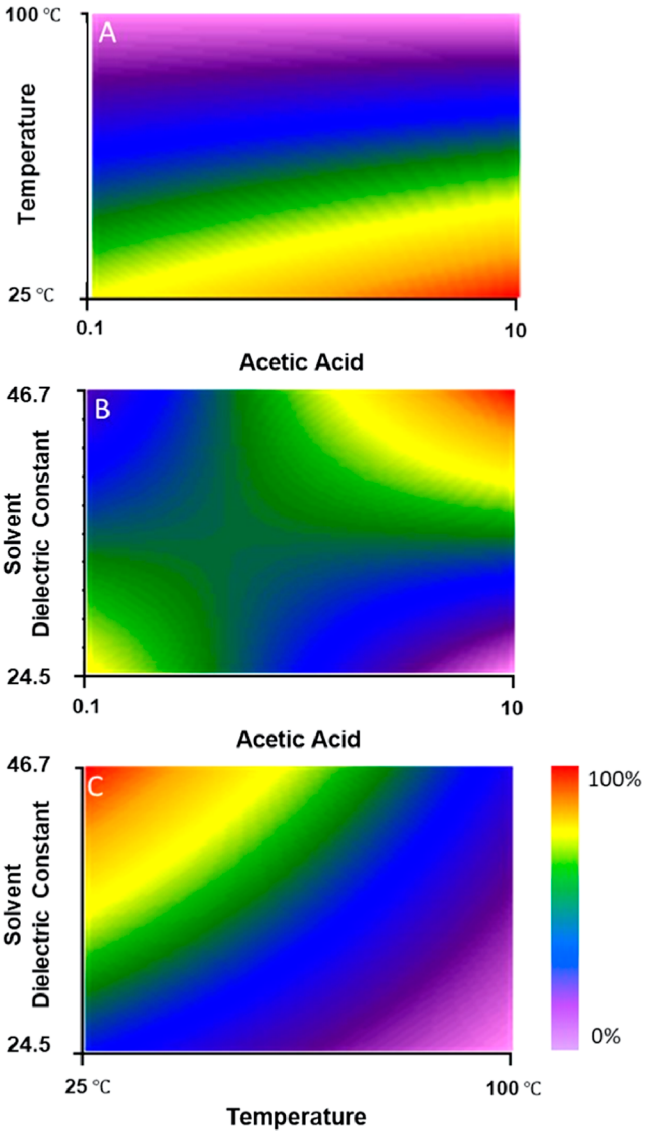

Figure 2. Contour plots derived from the analysis of DESI-MS data in 3^3 DoE-HTE. (A) Interaction of temperature with acetic acid equivalency, where the maximum point occurs at 25 °C and 10 equiv of acetic acid. (B) Interaction of solvent dielectric constant with acetic acid equivalency, where the maximum point occurs at 46.7 (DMSO) and 10 equiv of acetic acid. (C) Interaction of solvent dielectric constant with temperature, where the maximum point occurs at 46.7 (DMSO) and 25 °C.

Second Round of DoE and HTE

A second DoE was performed with a focus on A2E yield improvement and suppression of byproduct formation. After

https://doi.org/10.1021/acsbiomedchemau.1c00060
ACS Bio Med Chem Au 2022, 2, 297−306

analyzing the batch experiments that produced A2E in the literature, we observed that there are two different reagent stoichiometries utilized. While Parish et al.[5] utilizes a 2.27:1:1 ratio of ATR/ethanolamine/acetic acid, Guan et al.[21] utilizes a 1:19:24 ratio of ATR/ethanolamine: acetic acid.

In order to understand the role of each reagent in the synthesis of A2E, we designed another 3^3 factorial DoE, where the equivalence of each reagent was used as the minimum, intermediate, and maximum factors to generate a matrix of 27 unique experiments with DMSO as the solvent. We also sought to explore the effect of reaction temperatures on A2E yield, so that each set of 27 replicated experiments was performed at 25, 37, and 50 °C (we lowered the highest temperature in the experiments to 50 °C because the first DoE revealed that 100 °C was detrimental to A2E yield). Comparisons between the A2E product ion intensities produced by all 81 experiments indicates that the best reaction condition is 1 equiv of ATR, 10 equiv of ethanolamine, and 12 equiv of acetic acid at 25 °C (Table 2, run 23, 25 °C).

Table 2. HTE Results for the 3^3 DoE Equivalence Experiment[a]

run	equivalents ATR	EA	AA	% yield 25 °C	% yield 37 °C	% yield 50 °C
1	2.7	1	1	23.9	66.5	16.7
2	2.7	1	12	44.2	1.8	28.6
3	2.7	1	24	22.5	54.1	13.1
4	2.7	10	1	21.1	1.9	11.3
5	2.7	10	12	46.9	69.1	10.8
6	2.7	10	24	26.1	3.1	4.5
7	2.7	19	1	5.0	13.3	1.4
8	2.7	19	12	41.1	20.4	6.1
9	2.7	19	24	32.7	22.1	7.1
10	1.5	1	1	47.8	77.8	17.3
11	1.5	1	12	19.8	23.3	35.1
12	1.5	1	24	14.6	16.2	8.7
13	1.5	10	1	46.4	17.2	5.5
14	1.5	10	12	73.8	75.6	12.9
15	1.5	10	24	13.2	20.9	2.3
16	1.5	19	1	14.7	37.4	1.4
17	1.5	19	12	27.9	30.8	13.2
18	1.5	19	24	65.5	9.6	4.8
19	1	1	1	80.4	18.3	32.2
20	1	1	12	21.1	16.1	33.3
21	1	1	24	13.9	42.0	7.1
22	1	10	1	71.8	52.5	20.5
23	1	10	12	100.0	44.8	15.5
24	1	10	24	23.8	16.0	3.1
25	1	19	1	48.6	13.1	0.3
26	1	19	12	19.2	33.6	9.0
27	1	19	24	22.8	18.8	18.8

[a]ATR = all-trans retinal; EA = ethanolamine; and AA = acetic acid. % Yields are relative, as described above, and result from the average of the normalized ion intensities of the four replicates performed for each run at each temperature.

To gain a deeper understanding of the results obtained, we generated a Pareto analysis to detail the importance of each factor or combination of factors (Figure 3). The Pareto results reveal that the two most important factors are the interaction between ethanolamine/acetic acid equivalence and the interaction between ATR/acetic acid equivalence. Based on the mechanistic considerations for imine formation, we concluded that it was necessary to have a considerable amount of acid to enable leaving group formation, while retaining an effective concentration of free amine in solution to enable imine formation with the ATR aldehyde moiety.

Optimization of Continuous Flow Experiments

Using the results of the second HTE as a guide, we performed flow syntheses at two different flow rates—1 μL/min (i.e., a residence time, T_R, of 3.3 min) and 0.1 μL/min (T_R = 33 min). TLC analysis of the products clearly showed that increased residence time produced a more intense spot for the product and less intense spots for the byproducts, findings that were confirmed by product isolation after flash column chromatography (Table 3). The improved yield when the residence time is increased by an order of magnitude is related to the fact that the one-pot synthesis of A2E occurs over 48 h, such that a T_R = 3.3 min does not provide enough time for each step in the multistep transformation to occur. The maximum residence time possible for the experiment was achieved at 33 min due to the size limitations of the 3223 reactor and S1 system chosen for the study.

The flash column chromatography purified A2E produced a UV−vis spectrum (Figure 4A) with improved absorption bands than was obtained in the first round of flow experiments; however, it still did not produce the spectrum desired having a greater 439 nm band intensity.

LC−MS analysis (Figure S3) of the purified A2E isolated by a single flash column chromatography shows that the isolated A2E is still a mixture of over a dozen different compounds. The major peaks shown in the LC−MS data correspond to m/z 592 (A2E), another peak with m/z 592 (cis isomer), and m/z 608 (oxidized A2E).[22]

Based on this data, we tailored the conditions for preparative HPLC to produce a clear separation between the compounds in the mixture (ZORBAX ExtendC18 column, 9.4 × 250 mm, 5 μm, 80 A in a gradient of 85/25 to 95/5 ACN/H_2O for 1 h with a flow rate of 4 mL/min). A2E samples synthesized in flow and purified by this method gave a UV−vis spectrum with clear peaks at 331 and 440 nm (Figure 4B). Collectively, the UV−vis, NMR, and MS data indicate that pure A2E was obtained by this sequential flash and preparative HPLC method.

Scale-Up of A2E Synthesis in Flow

The flow setup used three syringe pumps to deliver the reagents, with ATR and ethanolamine first engaging in a T-mixer; that mixture then encounters acetic acid in a second T-mixer before flowing this final mixture through a coiled PFA tubing reactor (Figure 5).

Applying the optimized conditions derived from the microscale setup, we maintained the reagent equivalencies and residence time, but tested three different flow rates of 10, 5, and 2 μL/min while varying the length of the reactor tubing to maintain a consistent residence time. The fastest flow rate (10 μL/min) proved to be the most efficient (Table 4), a finding that can be attributed to improved mixing with the increase in flow rate.[23]

Pure A2E was obtained by collecting the reaction mixture from the flow reactor and isolating the product by sequential medium pressure liquid chromatography (MPLC) and preparative HPLC. The purity of A2E obtained is corroborated by the UV−vis spectrum obtained (Figure 6A), NMR (Figure S4), and LC−MS (Figure 6B). All data matched the results

https://doi.org/10.1021/acsbiomedchemau.1c00060
ACS Bio Med Chem Au 2022, 2, 297−306

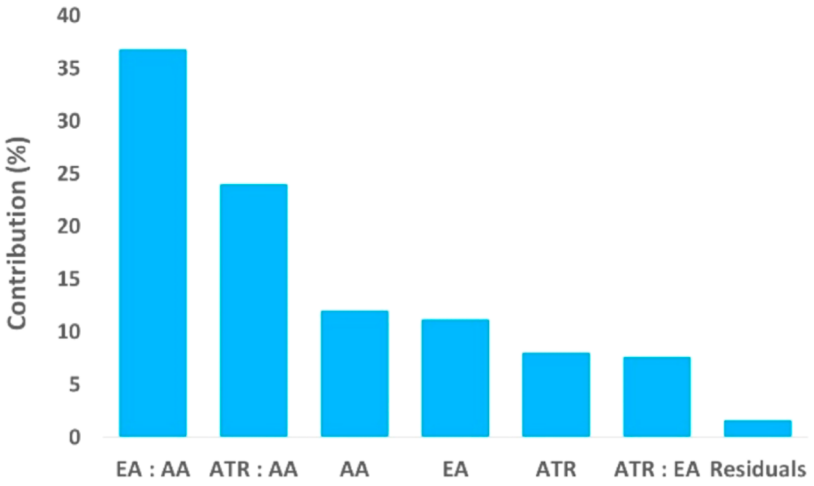

Figure 3. Pareto chart of the major effects impacting the yield of A2E. The red line represents the cumulative impact of the interactions.

Table 3. Continuous Flow Conditions Tested to Evaluate Residence Time Effects on A2E Yields (25 °C, DMSO)[a]

exp	equivalence ATR/EA/AA	flow rate (μL/min) ATR/EA/AA	residence time (T_R min)	A2E yield (%)
1	1:10:12	1:1:1	3.3	9
2	1:10:12	0.1:0.1:0.1	33	78

[a]ATR = all-*trans*-retinal (0.3 mol/L); EA = ethanolamine (3 mol/L); and AA = acetic acid (3.6 mol/L).

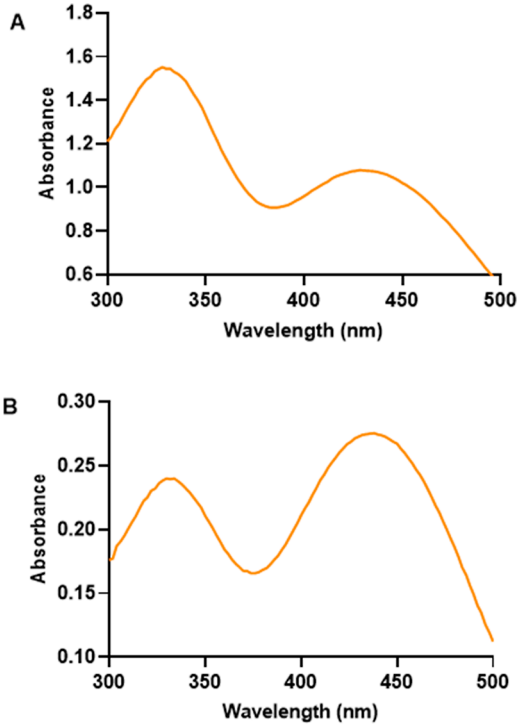

Figure 4. (A) UV−vis spectrum of A2E in MeOH after silica gel flash column chromatography purification using step gradient elution with 98:2:0.01 DCM/MeOH/TFA, 90:10:0.01 DCM/MeOH/TFA, and 2:1:0.01 DCM/MeOH/TFA, in sequence. (B) UV−vis spectrum of A2E in MeOH after preparative HPLC purification of the sample in (A) with a ZORBAX ExtendC18 column, 9.4 × 250 mm, 5 μm, 80 Å in a gradient of 85/25 to 95/5 ACN/H_2O for 1 h with a flow rate of 4 mL/min.

reported in the literature by Sparrow et al.[5] and Sicre and Cid,[24] but not Penn et al.[25]

As a further test of our method, we changed two parameters: residence time and solvent. In a first approach, we maintained the flow rate, reagent equivalences, temperature, and solvent, but increased the residence time fourfold, from 33 to 120 min (Table S3). The increased residence time only led to the increased production of byproducts, with a major UV−vis peak at 328 nm, a feature that is highly suggestive of increased A2-DHP-E content.[19,26] In the second case, we maintained the flow rate, residence time, reagent equivalences, and temperature, but used ethanol instead of DMSO. This reaction produced a far greater amount of iso-A2E than A2E (Table S4).

In order to develop an approach to rapidly assess and standardize A2E quality, we used absorption and fluorescence spectra. This method was extremely sensitive and easy for detecting differences in sample quality (Figure 7A,B). To understand the chemical basis underlying the spectral changes, we performed LC−MS analysis on the different A2E preparations (Figure 7C and Table S5). Two major m/z values were found for these samples: 592, corresponding to A2E, and 608, A2E's oxidized form. The ratio of oxidized and intact A2E's peaks was much larger in the case for Samples #1 (1:8) and #2 (1:3), compared to Sample #3 (1:62) derived from the scaled-up flow method that exhibited a minimal number of impurities. Although all A2E lots were toxic to RPE cells when fed in the dark for 24 h, the toxicities induced by oxidized lots #1 and #2 were partially protected by antioxidants (NAC), whereas intact A2E toxicity (A2E #3 and A2E #4) was better neutralized with the necroptosis inhibitor, Nec7.[27] Thus, the quality of the biological data generated with the different A2E lots was largely affected by the presence of even a small percentage of oxidized material (<5%) and to a lesser extent by residual ATR, leading to confounding biological results. This indicates the importance of the last purification step for the reliability of the biological response induced. Table 5 shows the concentrations of A2E inferred from the absorbance readings at 339 nm or 439 nm using the published molar extinction coefficients.[26] We found that the resulting concentrations from the 339 and 439 nm peaks from the same lot were only coincident when A2E was LC−MS pure and intact. This observation led us to calculate the 439/339 absorbance ratio as a measure of A2E sample

https://doi.org/10.1021/acsbiomedchemau.1c00060
ACS Bio Med Chem Au 2022, 2, 297−306

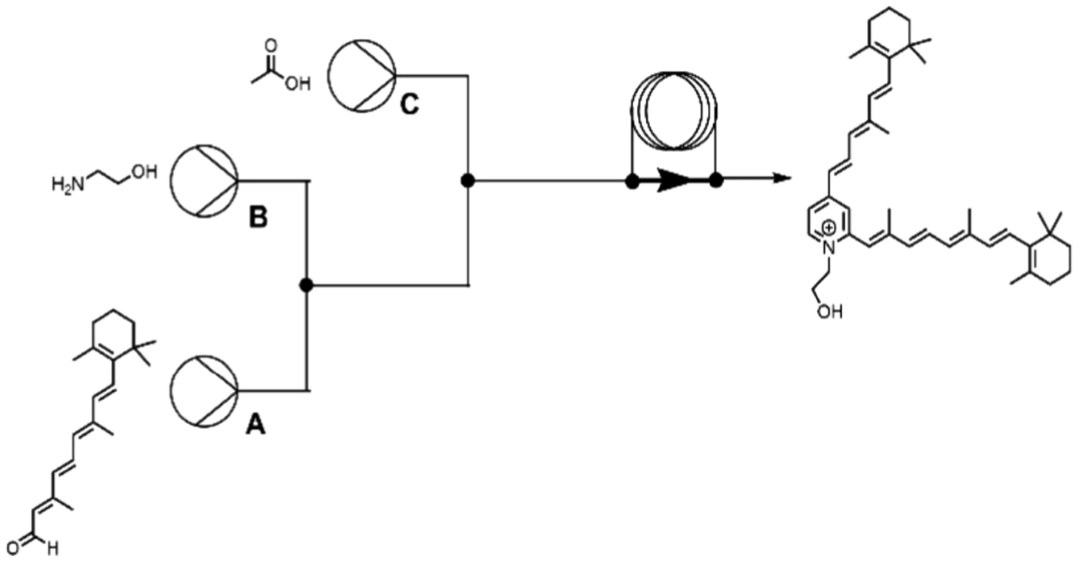

Figure 5. Continuous flow scale-up configuration. A: ATR, B: ethanolamine, and C: acetic acid.

Table 4. Upscaled Conditions for the Synthesis of A2E at 25 °C in DMSO at T_R = 33 min[a]

exp	equivalence ATR/EA/AA	flow rate (μL/min) ATR/EA/AA	A2E yield (%)
1	1:10:12	10:10:10	78
2	1:10:12	5:5:5	50
3	1:10:12	2:2:2	57

[a]ATR = all-trans retinal (0.3 mol/L); EA = ethanolamine (3 mol/L); and AA = acetic acid (3.6 mol/L).

quality. This index was low in oxidized or ATR-contaminated samples and increased to a maximum of 1.39 in A2E with the highest integrity and purity. Accordingly, the 439/339 ratio provided a way to easily rank the quality of the A2E preparations.

CONCLUSIONS

Based on conflicting literature reports about the synthesis methodology for A2E and the probable mechanism for A2E formation, we created two 3^3 DoEs that determined the best reaction conditions for the synthesis of A2E. DMSO, as reported by Jin et al.,[6] reduces the extent of A2E degradation as it is being formed. The ratio of acetic acid to ethanolamine also proved to be a significant factor for improving reaction yield. The reaction also proved to be sensitive to high temperatures, with more efficient reactions occurring at 25 °C.

After identifying the preferred reaction conditions, we synthesized A2E on small and large scales using continuous flow reactors. This modification reduced the reaction time from 48 h to 33 min of residence time, leading to a greatly improved A2E production. We also found that increased reaction time and EtOH as solvent lead to a greater byproduct formation. The most optimized condition for large production of A2E was achieved with a flow rate of 10 μL/min and a residence time of 33 min, utilizing DMSO as a solvent at 25 °C with an equivalence ratio of 1:10:12 of ATR/EA/AA. These conditions improved the isolated reaction yield from 49%[5] to 78%.

Finally, we investigated different purification methods in order to obtain A2E in the highest possible purity. Our findings suggest that a sequential MPLC and HPLC purification process generates highly pure A2E according to UV−vis, NMR, and LC−MS data. We also discovered that the sequential MPLC + HPLC purification sequence is crucial for obtaining A2E that produces reliably correct biological responses because the presence of even a small amount of oxidized species appears to result in variable biological performance.

EXPERIMENTAL METHODS

Reagents

AlamarBlue was from Invitrogen. All other reagents were purchased from Sigma-Aldrich and used without further purification.

NMR Analysis

NMR spectra were recorded using a Bruker AV-III-500-HD NMR spectrometer in CD_3OD and the chemical shifts reported versus TMS.

DESI-MS Analysis

High-throughput experiments and DESI-MS were performed using a previously published method.[14] In brief, a Biomek i7 liquid handling robot was used to prepare the reactions, and a LTQ XL (Thermo Scientific) fitted with a DESI two-dimensional stage (Prosolia Inc.) was used to analyze the reaction outcomes. After planning the experiment, the DoE matrix was transferred to a spreadsheet to be inputted on the Xcalibur software (version 3.0) for future use in the DESI-MS. Then, the reagents were transferred into 96-well heating blocks with the desired amounts (in pre-made solutions with the desired solvent). The heating blocks were set to the correct temperatures and, after 48 h (and cooling of the heating blocks to room temperature), the solutions were transferred to 384-well plates using the i7 robot. The DESI plates were pinned with the i7 robot and the DESI plate was analyzed with a linear ion trap mass spectrometer fitted with a DESI imaging source. The average ion counts for each combination in the matrix was replicated from three (HTE 2) to eight times (HTE 1) with its respective blank. The measured ion counts were averaged and normalized against the ion counts measured for the blank regions of the plate. The yields were calculated from the normalized average ion counts and the collected information was inputted into Ellistat software for statistical analysis.

Small-Scale Continuous Flow Synthesis of A2E

A2E was synthesized using continuous flow methodology in a Labtrix S1 system (Chemtrix BV, Echt, The Netherlands). Three 1 mL stock solutions of 99% DMSO containing ATR (0.3 mol/L, 85 mg),

https://doi.org/10.1021/acsbiomedchemau.1c00060
ACS Bio Med Chem Au 2022, 2, 297−306

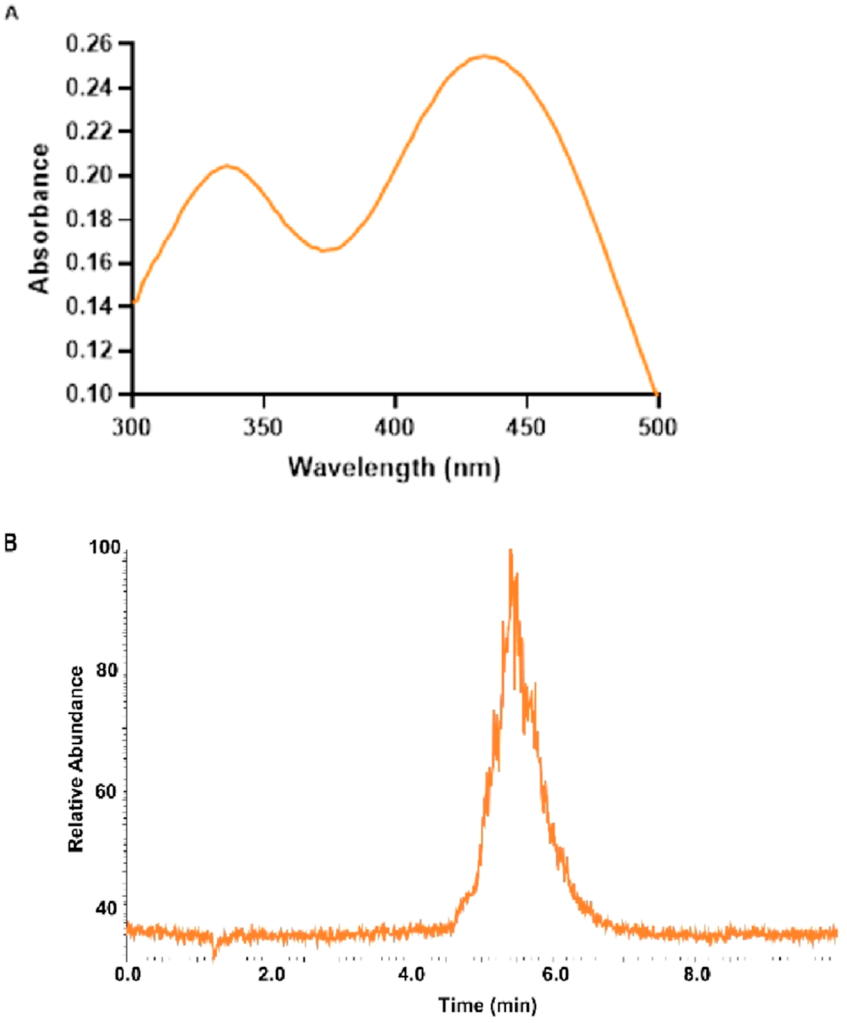

Figure 6. (A) Absorption spectrum obtained by sequential MPLC and preparative HPLC. LC−MS of A2E purified by flash column chromatography. (B) LC−MS was performed using an Eclipse XDB-C18, 4.6 × 150 mm, 5 μm, 30 °C, 95/5 ACN/H_2O with 0.1% TFA isocratically for 10 min with a flow rate of 1 mL/min.

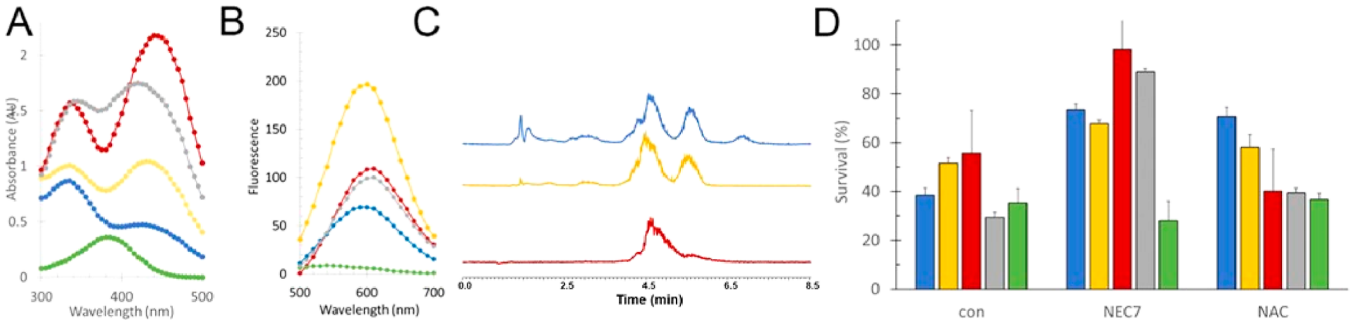

Figure 7. Comparison of three lots of A2E obtained during this study. A2E-#1 (blue); A2E-#2 (yellow); A2E-#3 (red); A2E-#4 (gray) is A2E#3 spiked with ATR at a 5:1 A2E/ATR molar ratio; and ATR (green) is shown for reference. A2E#3 was produced using the upscaled flow synthesis method reported here (Table 4, Exp 1). The combination of (A) absorbance spectra and (B) fluorescence spectra of the different lots provided a means to readily assess A2E quality. (C) LC−MS data show a dominant 592 Da peak in all the lots analyzed; however, in lots #1 and #2, there are extra peaks that based on their molecular weight likely represent heavily and moderately oxidized A2E, respectively.

ethanolamine (0.3 mol/L, 18 mg or 3 mol/L, 183 mg), and acetic acid (0.3 mol/L, 18 mg or 3 mol/L, 180 mg or 3.6 mol/L, 216 mg) were prepared, and the solutions were purged with Ar prior to being loaded into three 1 mL Hamilton syringes (Reno, NV), respectively. ATR and ethanolamine were added via a T junction into the same port of a staggered oriented ridge Chemtrix 3223 reactor chip (10 μL), with acetic acid added via a second port (see Figure S1). The syringes and chip were connected by FEP tubing (0.8 mm o.d. × 0.25 mm i.d., Dolomite Microfluidics). The respective flow rates are reported in Tables S1 and S2.

The reaction product solutions were extracted with ACN and washed five times with hexane and 1 M NaOAc. The ACN layer was dried under high vacuum. The resulting red solid was purified by silica gel column chromatography using a step elution with 98:2:0.01

https://doi.org/10.1021/acsbiomedchemau.1c00060
ACS Bio Med Chem Au 2022, 2, 297−306

Table 5. 439 nm/339 nm Absorption Ratio was the Parameter That can Most Readily Detect A2E Contamination with Oxidized Species or ATR[a]

	ABS(AU)		CC(mM)		
A2E#	339	439	339	439	RATIO 439/339
1	0.87	0.46	17.01	6.18	0.52
2	1.01	1.03	19.73	13.95	1.02
3	1.57	2.18	30.71	29.52	1.39
4	1.56	1.67	30.37	22.62	1.07

[a]Absorbance data were used to calculate the concentration of the A2E solutions based on published molar extinction coefficients of A2E at 339 and 439 nm.[24] Only highly purified A2E gave similar concentrations from either 339 or 439 OD values. The 439 nm/339 nm absorption ratio of 1.39 was the highest for pure A2E.

DCM/MeOH/TFA, 90:10:0.01 DCM/MeOH/TFA, and 2:1:0.01 DCM/MeOH/TFA, in sequence. The product fractions were further purified via semipreparative HPLC with a ZORBAX ExtendC18 column, 9.4 × 250 mm, 5 μm, 80 Å in a gradient of 85/25 to 95/5 ACN/H_2O for 1 h with a flow rate of 4 mL/min. The product fractions were flash-frozen and lyophilized. The resulting yields are reported in Tables S1 and S2.

Scaled-Up Continuous Flow Synthesis of A2E

Three 5 mL stock solutions of ATR (0.3 mol/L, 426 mg), ethanolamine (3 mol/L, 916 mg), and acetic acid (3.6 mol/L, 1081 mg) were prepared in 99% DMSO, and the solutions were purged with Ar prior to loading into three 25 mL Hamilton syringes, respectively. The syringes were mounted onto two Harvard syringe pumps and connected by FEP tubing (1/16 × 0.010 ft, IDEX) to the flow system according to Figure 5. The flow rates and R_T are described in Table 4.

After the reactions were complete, the product solutions were extracted with ACN and washed three times with 1 M NaOAc. The ACN layer was dried under high vacuum. The resulting red solid was purified by MPLC normal phase chromatography in gradient mode for 40 min, starting with 98:2:0.01 DCM/MeOH/TFA, until 50% MeOH with a flow rate of 15 mL/min. The product fractions were further purified via preparative HPLC with a Waters Prep C18 XBridge column, 30 × 100 mm, 10 μm, 80 Å in a gradient of 85/25 to 95/5 ACN/H_2O for 35 min with a flow rate of 40 mL/min. The product fractions were dried under reduced pressure. The resulting yields are reported in Table 4.

Cell Viability Assays

ARPE19 cells from ATCC were plated at 80% confluency in 96-well plates and pretreated for 1 h with inhibitors [33 μM Necrostatin 7 (Cayman Chemicals); 2 mM NAC (Sigma); and 50 μg/mL phoroglucinol (Sigma)] before supplementing the media with A2E/ATRD or vehicle (control) and incubating the cells in a serum-free OptiMEM (Invitrogen) medium for additional 23 h at 37 °C. To assess the viability, 20 μL of 10× AlamarBlue (Invitrogen) per well was added and cells were incubated by an additional hour before reading the fluorescence in SpectraMax M5e (Molecular Devices, CA, USA) using 555 nm excitation/585 nm emission.

UV/Vis Spectral Evaluation

A2E quality was assessed by diluting the A2E lot into ethanol. Absorbance and fluorescence spectra were determined in 96-well plates with black walls and clear bottoms. Absorbance was measured between 300 and 500 nm and fluorescence between 500 and 700 nm, with 410 nm excitation, using a Spectramax M5e.

LC–MS Analysis

LC–MS analysis was performed on a Quantum TSQ Discovery mass spectrometer (ThermoScientific) equipped with ThermoScientific autosampler, ThermoScientific mass spectrometry pump, and ThermoScientific ESI detector. Fifteen microliters of sample solution were loaded onto the column and eluted isocratically (mobile phase containing 95% acetonitrile, 5% water, and 0.1% TFA). The column used was an Agilent Eclipse XDB-C18 (4.8 × 150 mm) with a flow rate of 1 mL/min. The mass spectrometer was operated in the positive ion mode with a spray voltage at 5000 V and capillary at 350 °C. The Q1 quadrupole was scanned from m/z 50 to 1000.

■ ASSOCIATED CONTENT

Supporting Information

The Supporting Information is available free of charge at https://pubs.acs.org/doi/10.1021/acsbiomedchemau.1c00060.

NMR spectra, LC–MS spectra, high-resolution MS spectra, experimental setup, microscale continuous flow conditions before and after LC–MS, comparison between 33 and 120 min of residence time, comparison between DMSO and ethanol, and LC–MS analysis of A2E samples (PDF)

■ AUTHOR INFORMATION

Corresponding Author

David H. Thompson − *Department of Chemistry, Multidisciplinary Cancer Research Facility, Purdue University, West Lafayette, Indiana 47907, United States;* orcid.org/0000-0002-0746-1526; Email: davethom@purdue.edu

Authors

Giulia Murbach-Oliveira − *Department of Chemistry, Multidisciplinary Cancer Research Facility, Purdue University, West Lafayette, Indiana 47907, United States;* orcid.org/0000-0002-4863-3304

Kalpita Banerjee − *Weil Cornell Medical College, Ophthalmology Department, Dyson Research Institute, New York, New York 10065, United States*

Marcelo M. Nociari − *Weil Cornell Medical College, Ophthalmology Department, Dyson Research Institute, New York, New York 10065, United States*

Complete contact information is available at: https://pubs.acs.org/10.1021/acsbiomedchemau.1c00060

Author Contributions

The manuscript was written through contributions of all authors. All authors have given approval to the final version of the manuscript.

Notes

The authors declare no competing financial interest.

■ ACKNOWLEDGMENTS

This work was supported by the National Institute of Health, Grant # R01 EY027422 and by the CCSG Grant # P30 CA023168.

■ ABBREVIATIONS

A2E	*N*-retinylidene-*N*-retinylethanolamine
AA	acetic acid
ATR	all-trans-retinal
DoE	design of experiments
EA	ethanolamine
HTE	high-throughput experimentation
RPE	retinal pigment epithelium
ATRA	residence time

REFERENCES

(1) Kevany, B. M.; Palczewski, K. Phagocytosis of retinal rod and cone photoreceptors. *Physiology* **2010**, *25*, 8−15.

(2) Nociari, M. M.; Lehmann, G. L.; Perez Bay, A. E.; Radu, R. A.; Jiang, Z.; Goicochea, S.; Schreiner, R.; Warren, J. D.; Shan, J.; Adam de Beaumais, S.; Menand, M.; Sollogoub, M.; Maxfield, F. R.; Rodriguez-Boulan, E. Beta cyclodextrins bind, stabilize, and remove lipofuscin bisretinoids from retinal pigment epithelium. *Proc. Natl. Acad. Sci. U.S.A.* **2014**, *111*, E1402−E1408.

(3) Ben-Shabat, S.; Parish, C. A.; Vollmer, H. R.; Itagaki, Y.; Fishkin, N.; Nakanishi, K.; Sparrow, J. R. Biosynthetic studies of A2E, a major fluorophore of retinal pigment epithelial lipofuscin. *J. Biol. Chem.* **2002**, *277*, 7183−7190.

(4) Ben-Shabat, S.; Parish, C. A.; Hashimoto, M.; Liu, J.; Nakanishi, K.; Sparrow, J. R. Fluorescent pigments of the retinal pigment epithelium and age-related macular degeneration. *Bioorg. Med. Chem. Lett.* **2001**, *11*, 1533−1540.

(5) Parish, C. A.; Hashimoto, M.; Nakanishi, K.; Dillon, J.; Sparrow, J. Isolation and one-step preparation of A2E and iso-A2E, fluorophores from human retinal pigment epithelium. *Proc. Natl. Acad. Sci. U.S.A.* **1998**, *95*, 14609−14613.

(6) Jin, Q.-x.; Dong, X.-r.; Chen, J.-m.; Yao, K.; Wu, Y.-l. Effects of organic solvents on two retinal pigment epithelial lipofuscin fluorophores, A2E and all-trans-retinal dimer. *J. Zhejiang Univ., Sci., B* **2014**, *15*, 661−669.

(7) Laird, T. Design of experiments (DoE). *Org. Process Res. Dev.* **2002**, *6*, 337.

(8) Lendrem, D.; Owen, M.; Godbert, S. DOE (design of experiments) in development chemistry: Potential obstacles. *Org. Process Res. Dev.* **2001**, *5*, 324−327.

(9) Smallwood, H. M. Design of experiments in industrial research. *Anal. Chem.* **1947**, *19*, 950−952.

(10) Mills, J. E. Design of experiments in pharmaceutical process research and development. *ACS Symp. Ser.* **2003**, *870*, 87−109.

(11) Wleklinski, M.; Loren, B. P.; Ferreira, C. R.; Jaman, Z.; Avramova, L.; Sobreira, T. J. P.; Thompson, D. H.; Cooks, R. G. High throughput reaction screening using desorption electrospray ionization mass spectrometry. *Chem. Sci.* **2018**, *9*, 1647−1653.

(12) Loren, B. P.; Ewan, H. S.; Avramova, L.; Ferreira, C. R.; Sobreira, T. J. P.; Yammine, K.; Liao, H.; Cooks, R. G.; Thompson, D. H. High throughput experimentation using DESI-MS to guide continuous-flow synthesis. *Sci. Rep.* **2019**, *9*, 14745.

(13) Ewan, H. S.; Biyani, S. A.; DiDomenico, J.; Logsdon, D.; Sobreira, T. J. P.; Avramova, L.; Cooks, R. G.; Thompson, D. H. Aldol reactions of biorenewable triacetic acid lactone precursor evaluated using desorption electrospray ionization mass spectrometry high-throughput experimentation and validated by continuous flow synthesis. *ACS Comb. Sci.* **2020**, *22*, 796−803.

(14) Biyani, S. A.; Qi, Q.; Wu, J.; Moriuchi, Y.; Larocque, E. A.; Sintim, H. O.; Thompson, D. H. Use of high-throughput tools for telescoped continuous flow synthesis of an alkynylnaphthyridine anticancer agent, HSN608. *Org. Process Res. Dev.* **2020**, *24*, 2240−2251.

(15) Biyani, S. A.; Thompson, Y. W.; Moriuchi, D. H. Advancement in organic synthesis through high throughput experimentation. *Chem. Methods* **2021**, *1*, 323−339.

(16) Shevlin, M. Practical high-throughput experimentation for chemists. *ACS Med. Chem. Lett.* **2017**, *8*, 601−607.

(17) Mennen, S. M.; Alhambra, C.; Allen, C. L.; Barberis, M.; Berritt, S.; Brandt, T. A.; Campbell, A. D.; Castañón, J.; Cherney, A. H.; Christensen, M.; Damon, D. B.; Eugenio de Diego, J.; Garcia-Cerrada, S.; García-Losada, P.; Haro, R.; Janey, J.; Leitch, D. C.; Li, L.; Liu, F.; Lobben, P. C.; MacMillan, D. W. C.; Magano, J.; McInturff, E.; Monfette, S.; Post, R. J.; Schultz, D.; Sitter, B. J.; Stevens, J. M.; Strambeanu, I. I.; Twilton, J.; Wang, K.; Zajac, M. A.; Zajac, M. A. The evolution of high-throughput experimentation in pharmaceutical development and perspectives on the future. *Org. Process Res. Dev.* **2019**, *23*, 1213−1242.

(18) Plutschack, M. B.; Pieber, B.; Gilmore, K.; Seeberger, P. H. The Hitchhiker's Guide to Flow Chemistry. *Chem. Rev.* **2017**, *117*, 11796−11893.

(19) Wu, Y.-l.; Li, J.; Yao, K. Structures and biogenetic analysis of lipofuscin bis-retinoids. *J. Zhejiang Univ., Sci., B* **2013**, *14*, 763−773.

(20) Park, S.-i.; Park, S. C.; Kim, S. R.; Jang, Y. P. Two-step purification method for aging pigments A2E and iso-A2E using medium pressure liquid chromatography. *Bull. Korean Chem. Soc.* **2016**, *37*, 1541−1544.

(21) Guan, Z.; Li, Y.; Jiao, S.; Yeasmin, N.; Rosenfeld, P. J.; Dubovy, S. R.; Lam, B. L.; Wen, R. A2E distribution in RPE granules in human eyes. *Molecules* **2020**, *25*, 1413.

(22) Gutierrez, D. B.; Blakeley, L.; Goletz, P. W.; Schey, K. L.; Hanneken, A.; Koutalos, Y.; Crouch, R. K.; Ablonczy, Z. Mass spectrometry provides accurate and sensitive quantitation of A2E. *Photochem. Photobiol. Sci.* **2010**, *9*, 1513−1519.

(23) Samaddar, S.; Mazur, J.; Boehm, D.; Thompson, D. H. Development and in vitro characterization of bladder tumor cell targeted lipid-coated polyplex for dual delivery of plasmids and small molecules. *Int. J. Nanomed.* **2019**, *14*, 9547−9561.

(24) Sicre, C.; Cid, M. M. Convergent stereoselective synthesis of the visual pigment A2E. *Org. Lett.* **2005**, *7*, 5737−5739.

(25) Penn, J.; Mihai, D. M.; Washington, I. Morphological and physiological retinal degeneration induced by intravenous delivery of vitamin A dimers in rabbits. *Dis. Models Mech.* **2015**, *8*, 131−138.

(26) Sparrow, J. R.; Kim, S. R.; Wu, Y. Experimental approaches to the study of A2E, a bisretinoid lipofuscin chromophore of retinal pigment epithelium. *Methods Mol. Biol.* **2010**, *652*, 315−327.

(27) Pan, C.; Banerjee, K.; Lehmann, G. L.; Almeida, D.; Hajjar, K. A.; Benedicto, I.; Jiang, Z.; Radu, R. A.; Thompson, D. H.; Rodriguez-Boulan, E.; Nociari, M. M. Lipofuscin causes atypical necroptosis through lysosomal membrane permeabilization. *Proc. Natl. Acad. Sci. U.S.A.* **2021**, *118*, No. e2100122118.

https://doi.org/10.1021/acsbiomedchemau.1c00060
ACS Bio Med Chem Au 2022, 2, 297−306